NIH Public Access
Author Manuscript
Chem Commun (Camb). Author manuscript; available in PMC 2014 November 04.

Published in final edited form as:
Chem Commun (Camb). 2013 November 4; 49(85): . doi:10.1039/c3cc45000g.

CoCEST: Cobalt(II) Amide-Appended ParaCEST MRI Contrast Agents

Sarina J. Dorazio[a,§], **Abiola O. Olatunde**[a,§], **Joseph A. Spernyak**[b], and **Janet R. Morrow**[a]

Joseph A. Spernyak: joseph.spernyak@roswellpark.org; Janet R. Morrow: jmorrow@buffalo.edu

[a]Department of Chemistry, University at Buffalo, The State University of New York, Amherst, NY 14260, USA

[b]Department of Cell Stress Biology, Roswell Park Cancer Institute, Buffalo, NY14263, USA

Abstract

The first examples of air-stable Co^{II} paraCEST MRI contrast agents are reported. Amide NH protons on the complexes give rise to CEST peaks that are shifted up to 112 ppm from the bulk water resonance. One complex has multiple CEST peaks that may be useful for ratiometric mapping of pH.

The development of diagnostic probes for MRI based on biologically relevant transition metal ions is an emerging area of interest. Paramagnetic chemical exchange saturation transfer (paraCEST) MRI contrast agents are a relatively new class of contrast agent that contains d-block or f-block elements.[1] ParaCEST agents require a paramagnetic metal center which produces a large chemical shift of the exchangeable protons (NH, OH, or bound-H_2O) within the complex.[2] The selective irradiation of these labile protons partially saturates the proton spins which are in exchange with bulk water protons on the slow-to-intermediate NMR time regime.[3] This magnetization transfer gives rise to a decrease in the water signal for “on demand” MRI contrast. In choosing a paramagnetic metal ion, it is desirable to have poor proton relaxation enhancement (low relaxivity) and significant hyperfine shifts to reduce background interference from endogenous magnetization transfer in tissue.[4] Here we expand the class of transition metal-based paraCEST agents by introducing the first air stable Co^{II} paraCEST (CoCEST) agents. Co^{II} is one of the most well-known transition metal paramagnetic shift agents, and these properties make it well-suited for paraCEST MRI contrast.[5] We show that amide pendent groups attached to several different azamacrocycles bind Co^{II} to give CoCEST agents with unique MRI contrast properties.

Co^{II} complexes of four different macrocycles were prepared (Scheme 1). Solution magnetic moments for $[Co(1)]^{2+}$, $[Co(2)]^{2+}$, $[Co(3)]^{2+}$, and $[Co(4)]^{2+}$ are 5.2, 4.5, 4.6, and 4.1 μ_B, respectively, at 25 °C in D_2O, suggestive of high spin (HS) Co^{II}(S = 3/2).[6] In the absence of dynamic processes, the Co^{II} complexes have fairly narrow proton resonances at full width half maximum (FWHM), corresponding to the short electronic longitudinal relaxation time (T_{1e}) of HS Co^{II}.[4a] The 12 distinct narrow proton resonances (FWHM = 70–350 Hz) of $[Co(4)]^{2+}$ in D_2O correspond to the number expected for a complex with two coordinated pendent amides bound *trans* to give local C_2 symmetry (Figure S1). This is consistent with a

Correspondence to: Janet R. Morrow, jmorrow@buffalo.edu.

[7]Both authors contributed equally.

[†]Electronic Supplementary Information (ESI) available: [details of any supplementary information available should be included here]. See DOI: 10.1039/b000000x/

NIH-PA Author Manuscript
NIH-PA Author Manuscript
NIH-PA Author Manuscript

NIH-PA Author Manuscript

NIH-PA Author Manuscript

NIH-PA Author Manuscript

pentagonal bipyramidal coordination environment as shown for a Co^{II} complex of a similar ligand.[7]

$[Co(3)]^{2+}$ also displays relatively narrow ^1H NMR resonances (FWHM = 70–500 Hz), although the spectrum is complicated by a small percentage of a minor isomer (~ 4 %) (Figure S2). Several different conformations may be adopted by transition metal ion complexes of tetrasubstituted cyclam derivatives including isomers that have two pendent groups bound either *trans* or *cis*.[9] The large number of proton resonances for the major isomer of $[Co(3)]^{2+}$ suggests that the complex lacks any symmetry, which is most consistent with *cis*-pendent groups. In contrast, broad and fairly indistinguishable resonances are observed for $[Co(1)]^{2+}$ and $[Co(2)]^{2+}$ (Figures S3 and S4). These broad NMR spectral features are produced by dynamic processes on the NMR time-scale which make it difficult to determine solution coordination number and geometry.[1a,b] In the solid state, $[Co(1)]^{2+}$ is shown to have a hexadentate ligand as supported by spectroscopic methods.[10] The crystal structure of $[Mn(2)]Cl_2{\cdot}2H_2O$ shows an octadentate macrocycle.[11] However, the macrocycle in $[Co(2)]^{2+}$ may be octadentate or of lower denticity based on the smaller ionic radius of HS Co^{II} in comparison to HS Mn^{II}.

To gauge the feasibility of studying these compounds *in vivo*, the kinetic inertness of the prepared Co^{II} complexes was monitored by using ^1H NMR spectroscopy. The diamagnetic region of the NMR spectra was monitored in the presence of a standard after 12 h incubation at 37 °C. In the presence of physiologically relevant concentrations of phosphate (0.40 mM) and carbonate (25 mM) at near-neutral pD, the dissociation of all complexes was minimal (Table 1 and Figures S5 – S8). Acidic conditions (pD 3.5 – 3.9) gave more variable results. At the two extremes, dissociation of $[Co(1)]^{2+}$ was insignificant at only 1% over 12 h, while $[Co(3)]^{2+}$ dissociated 95% within the first hour. $[Co(2)]^{2+}$ and $[Co(4)]^{2+}$ were moderately inert at 7% and 16% dissociation, respectively (Table 1 and Figures S9 – S12). Dissociation of the complexes was also studied by addition of a 10-fold excess of Cu^{II} as a competing metal ion and monitoring the formation of the Cu^{II} complex through UV-vis spectroscopy. While $[Co(2)]^{2+}$ is inert to dissociation, $[Co(1)]^{2+}$ dissociates approximately 15% over 4 h. $[Co(3)]^{2+}$ and $[Co(4)]^{2+}$ are significantly more labile, dissociating completely within 1 h.

CEST NMR spectra were produced using an 11.7 T NMR spectrometer through a presaturation experiment plotted as normalized water signal intensity (M_z/M_o %) against frequency offset (ppm). Saturation times of 2–4 s gave similar CEST intensities (Figure S13). Notably, restricted C-N bond rotation of the amide groups in these complexes yields two magnetically inequivalent NH protons on an amide group.[12] For example, $[Co(4)]^{2+}$ has two highly separated CEST peaks at 59 and −19 ppm assigned to two magnetically inequivalent amide protons on two symmetry-related pendent groups. The single observed CEST peaks for $[Co(1)]^{2+}$ or $[Co(2)]^{2+}$ are shifted away from bulk water at 32 and 45 ppm, respectively (Figure 1a). The second amide proton resonance is either not sufficiently shifted to distinguish it from the water peak or has a rate constant for exchange which is not conducive for observation of a CEST peak. $[Co(3)]^{2+}$ exhibits four CEST peaks (112, 95, 54, and 45 ppm) of similar intensity and a smaller CEST peak at −15 ppm (Figure 1b). The simplest assignment of the four distinct major CEST peaks is to two bound amide pendents that are not symmetry related.

CEST intensities increased for all complexes over the pH range of 6.5–7.5, consistent with base-catalyzed amide exchange (Figure S14, S15), with optimal CEST intensities at pH 7.5–7.7. Rate constants for proton exchange at pH 7.4 varied from 240 to 910 s^{-1} (Table 1 & Table S1). These rate constants, together with the CEST versus pH curves, are supportive of their assignment as amide protons. Similar CEST properties are observed for Fe^{2+} and Ln^{3+} complexes with pendent amide groups.[1,13a] Interestingly, the two most highly shifted peaks

NIH-PA Author Manuscript

NIH-PA Author Manuscript

NIH-PA Author Manuscript

of $[Co(3)]^{2+}$ at 112 and 95 ppm have distinct pH dependencies. A ratiometric plot of the CEST effect of the two peaks versus pH is linear, showing that this agent is promising for ratiometric pH mapping (Figures 1b & 1c).

CEST MR phantom images were acquired on a 4.7 T scanner using a phantom array containing solutions of 0.25, 0.50, 0.75, 1.0 or 4.0 mM Co^{II} complex, 100 mM NaCl, 20 mM buffer pH 7.4 at 37 °C (Figure 1d). A pair of gradient echo images was acquired with a presaturation pulse either on-resonance or off-resonance of the exchangeable protons (59/−59 ppm for $[Co(4)]^{2+}$, 45/−45 ppm for $[Co(2)]^{2+}$, 32/−32 ppm for $[Co(1)]^{2+}$ and either 112/−95ppm or 95/−95 ppm for $[Co(3)]^{2+}$. The ratio between these two images is subtracted from 100% to generate a CEST image. The phantoms show that the CEST effect increases with the concentration of the Co^{II} complex over the range 0.25 to 4.0 mM (Figure S16).

The CoCEST phantom images at 4 mM agent (5 – 12 %) show that the most intense CEST effect belongs to $[Co(4)]^{2+}$ and $[Co(2)]^{2+}$. The CEST effect for these two complexes is similar, despite the fact that there are half the number of amide NH protons for $[Co(4)]^{2+}$ as for $[Co(2)]^{2+}$ and both have similar k_{ex}. Notably, the T_1 relaxivities for $[Co(4)]^{2+}$ and $[Co(3)]^{2+}$ are low, and this may contribute to an enhanced CEST effect (Table 2).[13]

CEST MR phantom images of $[Co(3)]^{2+}$ were obtained as a function of pH for the furthest shifted CEST peaks (112 ppm and 95 ppm) to further validate ratiometric pH contrast properties. In order to improve data precision by averaging multiple data points, images were obtained by using CEST FISP (FISP = fast imaging with steady-state free precession) protocol. As FISP imaging allows for the acquisition of the entire MR image after the CEST presaturation pulse, 20 CEST image data points were acquired in less than 2 minutes to greatly shorten data collection time. A plot of the ratio of CEST signal (112:95 ppm) vs. pH shows a linear relationship (Figure S17), analogous to the CEST NMR experiments (Figure 1c).

Conclusions

In summary, the first series of air stable CoCEST agents are formed from azamacrocycles containing pendent amide groups. All complexes are moderately inert towards dissociation in the presence of biologically relevant anions, while ligands 1 and 2 give the most inert Co^{II} complexes under acidic conditions or with competing transition metal ions. The diverse coordination chemistry of Co^{II} leads to the production of one, two or five CEST peaks with shifts ranging from −19 ppm to 112 ppm. Notably, the multiple CEST peaks produced by $[Co(3)]^{2+}$ facilitate the development of ratiometric agents by using the distinct pH dependence of two different protons. This simplifies the synthesis of ratiometric paraCEST agents because it eliminates the need to add different pendent groups. These examples show that CoCEST agents are a valuable addition to the class of paramagnetic transition metal ion- based CEST contrast agents.

Supplementary Material

Refer to Web version on PubMed Central for supplementary material.

Acknowledgments

We gratefully acknowledge the John R. Oishei Foundation, the Bruce 70 Holm Catalyst Fund and the NIH (CA-173309) for support. MR imaging was supported in part by Roswell Park's NCI Support Grant (P30CA16056) and the Roswell Park Alliance Foundation. We thank Michael Daddario and Steven Turowski for assisting with imaging experiments.

NIH-PA Author Manuscript

NIH-PA Author Manuscript

NIH-PA Author Manuscript

Notes and references

1. (a) Dorazio SJ, Tsitovich PB, Siters KE, Spernyak JA, Morrow JR. J. Am. Chem. Soc. 2011; 133(36):14154–14156. [PubMed: 21838276] (b) Dorazio SJ, Morrow JR. Inorg. Chem. 2012; 51(14):7448–7450. [PubMed: 22757664] (c) Tsitovich PB, Morrow JR. Inorganica Chim. Acta. 2012; 393:3–11.(d) Olatunde AO, Dorazio SJ, Spernyak JA, Morrow JR. J. Am. Chem. Soc. 2012
2. Viswanathan S, Kovacs Z, Green KN, Ratnakar SJ, Sherry AD. Chem. Rev. 2010; 110(5):2960–3018. [PubMed: 20397688]
3. Woods M, Woessner DE, Sherry AD. Chem. Soc. Rev. 2006; 35(6):500–511. [PubMed: 16729144]
4. (a) Bertini I, Luchinat C, Parigi G, Pierattelli R. ChemBioChem. 2005; 6(9):1536–1549. [PubMed: 16094696] (b) Dorazio SJ, Morrow JR. Eur. J. Inorg. Chem. 2012; 12:2006–2014.
5. Bertini, I.; Luchinat, C. NMR of Paramagnetic Molecules in Biological Systems. Menlo Park: The Benjamin/Cummings Publishing Company, Inc.; 1986.
6. Crabb, E.; Moore, E.; Smart, L. Concepts in Transition Metal Chemistry. Cambridge, United Kingdom: Royal Society of Chemistry Open University; 2010.
7. (a) Vaiana L, Regueiro-Figueroa M, Mato-Iglesias M, Platas-Iglesias C, Esteban-Gomez D, de Blas A, Rodriguez-Blas T. Inorg. Chem. 2007; 46(20):8271–8282. [PubMed: 17764174] (b) Regueiro-Figuero M, Esteban-Gomez D, Platas-Iglesias C, de Blas A, Rodriguez-Blas T. Eur. J. Inorg. Chem. 2007; 15:2198–2207.
8. (a) Evans DF. J. Chem. Soc. 1959:2003–2005.(b) Schubert EM. J. Chem. Ed. 1992; 69(1):62.
9. Ozay H, Baran Y, Ishii Y. Spectrochim. Acta, Part A. 2011; 83(1):525–531.
10. Weyhermuller T, Wieghardt K, Chaudhuri P. J. Chem. Soc. Dalton Trans. 1998; 22:3805–3813.
11. Wang S, Westmoreland TD. Inorg. Chem. 2009; 48(2):719–727. [PubMed: 19072697]
12. Ming LJ, Lauffer RB, Que L Jr. Inorg. Chem. 1990; 29(16):3060–3064.
13. (a) Aime S, Delli Castelli D, Terreno E. Angew. Chem. Int. Ed. 2002; 41(22):4334–4336.(b) Zhang S, Merritt M, Woessner DE, Lenkinski RE, Sherry AD. Acc. Chem. Res. 2003; 36(10): 783–790. [PubMed: 14567712]

NIH-PA Author Manuscript
NIH-PA Author Manuscript
NIH-PA Author Manuscript

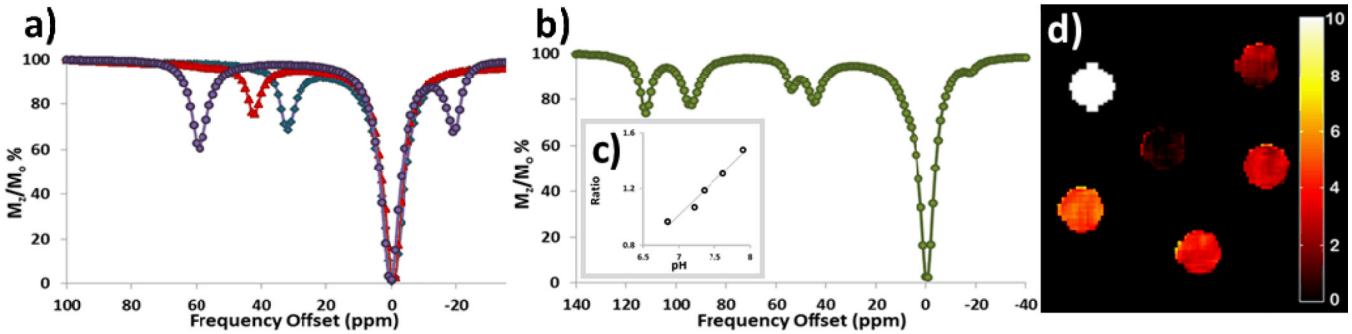

Figure 1.

a) Overlaid CEST spectra of 10 mM (purple circle = $[Co(4)]^{2+}$); (red triangle = $[Co(2)]^{2+}$) ; (blue diamond = $[Co(1)]^{2+}$), 20 mM HEPES, B_1= 24 μT for 2s at 37 °C. **b)** CEST spectrum of 10 mM $[Co(3)]^{2+}$, B_1= 24 μT for 2 s at 37 °C. **c)** Ratiometric plot of 10 mM $[Co(3)]^{2+}$, B_1= 24 μT for 2 s with pH of 6.8–7.8 giving slope of 0.49. The y-axis "Ratio" is the ratio of $[1-(M_z/M_o)]$ at 112 ppm to $[1-(M_z/M_o)]$ at 95 ppm. **d)** CEST images of phantoms on a MRI 4.7 T scanner with a pulse train comprised of five Gauss pulses at 12 μT for 1 s each, interpulse delay of 200 μs applied symmetrically about the bulk water resonance (+/− 59 ppm) for $[Co(4)]^{2+}$ at 0.25, 0.50, 0.75, 1.0, 4.0 mM. Scale bar represents CEST signal $(1-M_z/M_o)$. Samples are arranged in increasing concentration from the "one o'clock" position, clockwise. Center contains buffer and NaCl only. All samples contained 20 mM HEPES buffer, 100 mM NaCl, pH 7.4 (except where noted) at 37 °C.

NIH-PA Author Manuscript

NIH-PA Author Manuscript

NIH-PA Author Manuscript

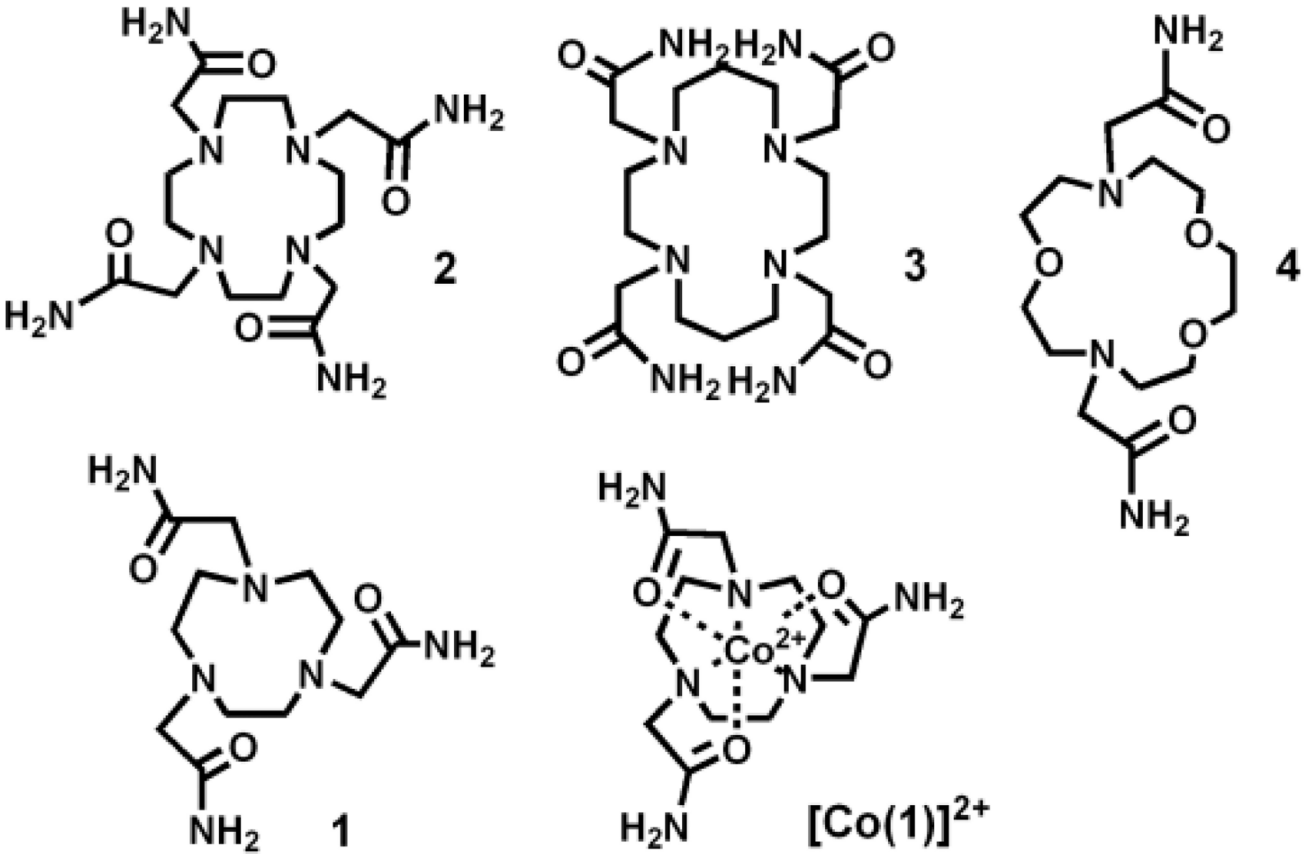

Scheme 1.
Ligands and an example of a Co^{II} paraCEST agent.

NIH-PA Author Manuscript
NIH-PA Author Manuscript
NIH-PA Author Manuscript

Table 1

Effective magnetic moment and dissociation of Co^{II} complexes in D_2O solutions at 37 °C.

Complex	μ_{eff}[a] μ_B	% Dissociation[b] Acidic	% Dissociation[c] Anions
$[Co(1)]^{2+}$	5.2	1	5
$[Co(2)]^{2+}$	4.5	7	2
$[Co(3)]^{2+}$	4.6	95	5
$[Co(4)]^{2+}$	4.1	16	<1

[a] 5 mM Co^{II} complex in D_2O.[1a, 8]

[b] pD 3.5 – 3.9, 100 mM NaCl, 12 h incubation at 37 °C.

[c] 0.40 mM Na_2HPO_4, 25 mM K_2CO_3, 100 mM NaCl, pD 7.5 – 7.9, 12 h incubation at 37 °C.

NIH-PA Author Manuscript

NIH-PA Author Manuscript

NIH-PA Author Manuscript

Table 2

Rate constants, relaxivity and CEST effect of CoCEST agents with 20 mM HEPES buffer and 100 mM NaCl,

Complex	k_{eff}[a] (s^{-1})	T_1 Relaxivity [b] ($mM^{-1}·s^{-1}$)	T_2 Relaxivity[c] ($mM^{-1}·s^{-1}$)	% CEST[d]
$[Co(1)]^{2+}$	890	0.125	0.297	8
$[Co(2)]^{2+}$	300	0.096	0.213	12
$[Co(3)]^{2+}$	510[e],910[f]	0.008	0.127	8[e],5[f]
$[Co(4)]^{2+}$	240	0.038	0.119	12

[a] Proton exchange rate constant (k_{ex}) obtained on 11.7 T spectrometer with 10 mM CoCEST agent and B_1 varied between 8 and 24 μT, 4 s, 37 °C.

[b,c] T_1 and T_2 relaxivities, respectively, acquired at 4.7 Telsa, 37 °C for 0.25 – 4 mM CoCEST complex, pH 7.4 – 7.5 using an inversion-recovery TrueFISP relaxometry protocol (T_1) and a Carr-Purcell-Meiboom-Gill multi-echo echo sequence (T_2).

[d] % CEST of 4 mM CoCEST agent, pH 7.4 – 7.5, 37 °C on a 4.7 T MRI scanner.

[e] % CEST for peak at 112 ppm

[f] peak at 95 ppm.